Cabral, A.R., et al., 2021, Extreme fractionation of selenium isotopes and possible deep biospheric origin of platinum nuggets from Minas Gerais, Brazil: Geology, v. 49, https://doi.org/10.1130/G49088.1

Supplemental Material

Extreme fractionation of selenium isotopes and possible deep biospheric origin of platinum nuggets from Minas Gerais, Brazil

Alexandre Raphael Cabral[1,2*], Stephan König[3,4*], Benjamin Eickmann[3,5], Michael Brauns[6], Miguel Tupinambá[7], Bernd Lehmann[8], and María Isabel Varas-Reus[3]

[1]Centro de Pesquisa Professor Manoel Teixeira da Costa, Instituto de Geociências, Universidade Federal de Minas Gerais (UFMG), Belo Horizonte-MG, 31270-901, Brazil
[2]Centro de Desenvolvimento da Tecnologia Nuclear (CDTN), Belo Horizonte-MG, 31270-901, Brazil
[3]Isotope Geochemistry, Department of Geosciences, University of Tübingen, 72076 Tübingen, Germany
[4]Instituto Andaluz de Ciencias de la Tierra (IACT), Consejo Superior de Investigaciones Científicas and Universidad de Granada, Avenida las Palmeras 4, Armilla, 18100 Granada, Spain
[5]Departamento de Geociencias, Universidad de los Andes, Carrera 1#18A-12, 111711 Bogotá, Colombia
[6]Curt-Engelhorn-Zentrum Archäometrie (CEZA), 68159 Mannheim, Germany
[7]Tektos–Geotectonic Research Group, Faculdade de Geologia, Universidade do Estado do Rio de Janeiro, Rio de Janeiro-RJ, 20550-050, Brazil
[8]Mineral Resources, Technische Universität Clausthal, Adolph-Roemer-Strasse 2a, 38678 Clausthal-Zellerfeld, Germany

*Corresponding authors, E-mails: arcab@ufmg.br; skonig@gmx.de

METHODS

Isotope measurements of Se from Pt-Pd nuggets were performed following the protocol described by Kurzawa et al. (2017) and Yierpan et al. (2018). For this, sample material is mixed with a ^{74}Se-^{77}Se double spike and digested in concentrated HCl:HNO_3 1:1 (v/v) in closed beakers on a hotplate at 85°C for 48 hours. To assure complete digestion, we additionally digested two specimens in an AntonPaar High pressure Asher (HPA, Yierpan et al., 2018). Selenium is purified from trace Fe via anion exchange chromatography according to the procedure previously used for pyrite (König et al., 2019). Selenium isotopic compositions were determined, using a ThermoFisher Scientific Neptune^{Plus} MC–ICP–MS, by hydride generation and in low-resolution mode at the Isotope Geochemistry laboratory, University of Tübingen. Typical signals on ^{82}Se, with an amplifier resistor of 10^{11} Ω, on a Se solution of 30 ng mL^{-1}, and operating parameters similar to those reported in (Kurzawa et al., 2017), were generally 0.8–0.9 V. Selenium isotopes of samples were determined at similar signal intensities compared to those of standard solutions.

For detailed descriptions of analytical techniques employed, see Yierpan et al. (2018) and Kurzawa et al. (2017).

Platinum-poisoning effects on H_2Se formation in the hydride generator (Bolea et al., 2001), and unknown but potentially related Se isotopic fractionation are corrected for by the double-spike method employed here. All Se isotopic compositions obtained during this study are reported relative to the NIST-3149 Se reference solution (delta-zero-anchor). Measurements of the inter-laboratory standard solution MH-495 in four different analytical sessions over a period of more than 6 months yielded an average value of $\delta^{82/76}Se$ of -3.23 ± 0.15 ‰ (2 SD, N = 23, 30 ng mL^{-1} solutions, Table S3), in agreement with previous studies (Kurzawa et al., 2017, 2019; Labidi et al., 2018; Yierpan et al., 2018, 2019), and our long-term reproducibility in our lab over 5 years. International rock reference material USGS BCR-2 was repeatedly digested and analyzed during the course of this study, and gave $\delta^{82/76}Se$ of 0.14 ± 0.15 ‰ (2 SD, N = 4) and Se concentration of 78 ng g^{-1}, respectively (Table S4, see also König et al., 2021). This is in agreement with previously published Se concentration and isotope composition (Kurzawa et al., 2017; Yierpan et al., 2018, 2019). A detailed compilation of reference-material data, further documenting the accuracy and reproducibility of our Se-isotope method, are openly accessible (Yierpan et al. 2020, and supplemental material therein). Long-term analytical reproducibility for determination of Se concentration is ~3% (1 SD). Measurements of nuggets after both hotplate beaker and HPA digestion produced similar results. Since no Pt-Pd materials exist as references for Se isotopes, we report a conservative external reproducibility of $\delta^{82/76}Se$ for these samples as 0.2 ‰ (2 SD), compared to that obtained for low Se abundance, mafic reference materials (Yierpan et al., 2020).

Measurements for Os isotopes were carried out following the method previously described in (Brauns et al., 2000, 2001). In this study, Pt-Pd nuggets of 1–7 mg were placed into pre-spiked (^{190}Os-tracer) Carius tubes, followed by dissolution and equilibration with 4 ml of inverse aqua regia at 240 °C. Osmium was extracted by distillation of the volatile tetroxide, condensed in 20 µl of chilled H_2SO_4 and then collected in 1.5 ml of 6.8 N HBr. Final purification of Os was achieved by microdistillation (Birck et al., 1997). Isotopic ratios of Os were measured by ion-counting on a modified Finnigan-MAT 261 mass spectrometer operated in NTIMS mode, corrected for mass bias and oxides. Internal (2 SD) precision for unknowns was <0.2 %. Final $^{187}Os/^{188}Os$ ratios were corrected for blank (0.1–0.05 pg Os, $^{187}Os/^{188}Os$ blank of 0.108), assuming an Os yield of 85 % (Brauns et al., 2020). Blank contribution for samples with low Os concentrations are less than 0.5%. During the course of this study, the reference material JM-Os-DTM yielded an average $^{187}Os/^{188}Os$ ratio of 0.17393 ± 38 (N = 7), which is consistent with published results (see Table S1 for details). Final $^{186}Os/^{188}Os$ ratios, as basis for determining ^{186}Os concentrations, were calculated using a modified data reduction scheme of (Birck et al., 1997). Concentrations of Pt and Pd were determined on the solution directly taken from the Carius tube, by means of an ICap Q (Thermo QICP MS), in two different ways: normalizing Pt

and Pd to 100; and directly measuring Pt and Pd using a calibration curve. The results are, within error, identical. Each Pt-Pd nugget had its Pt-Os age calculated according to the equation:

$$1/(1.477*10^{-12})*LN((^{186}Os_{sample}/^{190}Pt_{sample})+1)/10^{6},$$

the decay constant of which comes from Begemann et al. (2001).

SUPPLEMENTAL FIGURE

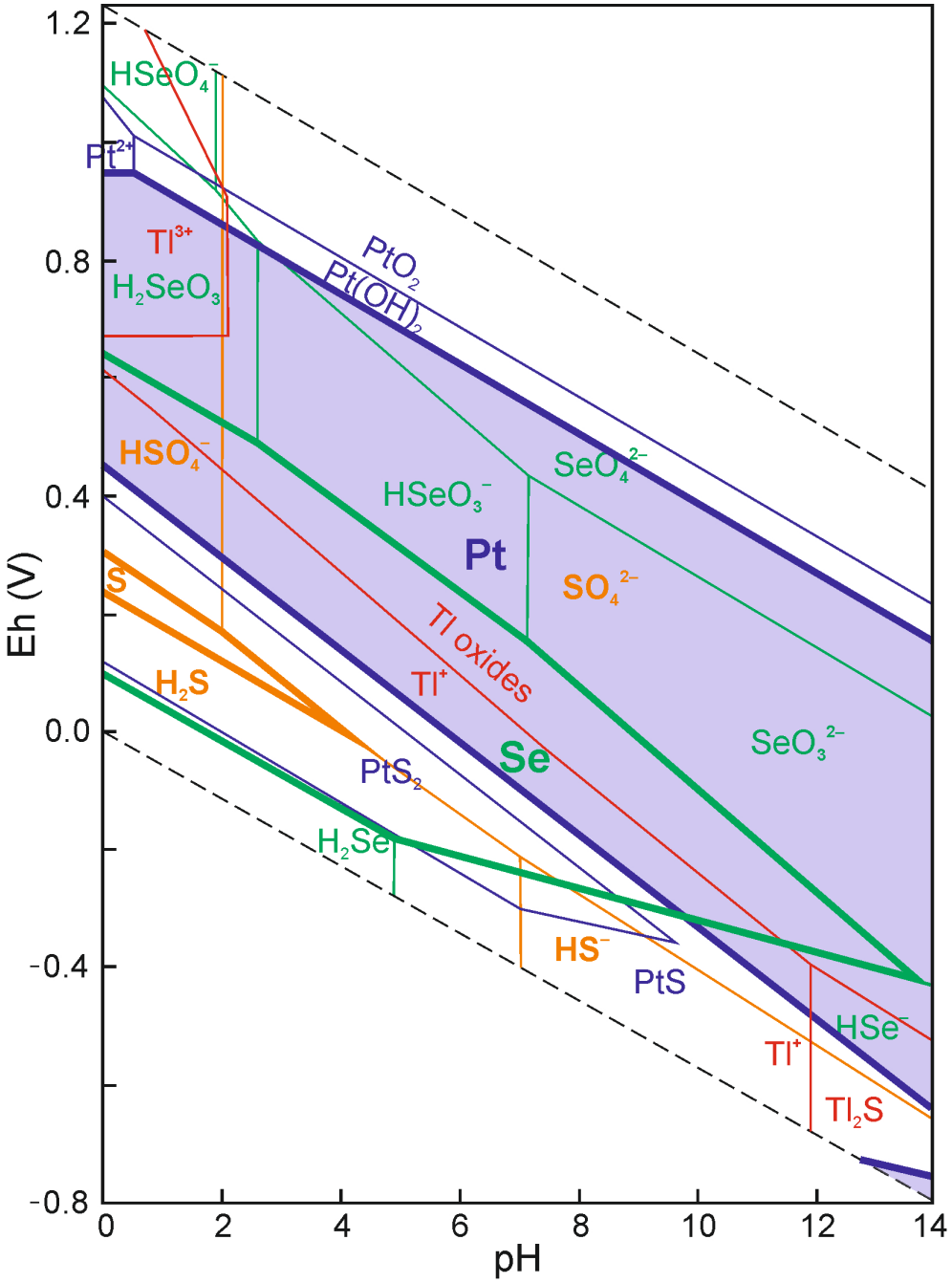

Fig. S1. Superposition of Eh-pH diagrams at 25 °C for S, Se, Pt and Tl species (Brookins, 1988). Note that elemental Tl is not indicated because it is stable below the lower limit of water stability (dashed line intercepting the pH and Eh axes at 14 and 0.0, respectively). The stability field of elemental Pt, shaded in blue, overlaps with that of elemental Se, delimited by thick line in green.

SUPPLEMENTAL TABLES

TABLE S1. PLATINUM-OSMIUM AGES FOR PLATINUM-PALLADIUM NUGGETS FROM CÓRREGO BOM SUCESSO, MINAS GERAIS, BRAZIL

Sample	^{186}Os (ng g^{-1})*	Common Os (ng g^{-1})	$^{186}Os/^{188}Os$	2 SD	$^{187}Os/^{188}Os$	2 SD	Pt (wt.%)	$^{190}Pt/^{186}Os$ age (Ma)	2 SD
Serro 1	24	8	10.865	0.043	1.301	0.005	72.1	179.1	7.2
Serro 6	26	15	7.481	0.030	0.896	0.004	82.7	174.4	7.0
Serro 8	24	12	7.854	0.031	0.940	0.004	72.6	184.7	7.4
Serro 9	23	10	10.825	0.043	1.296	0.005	69.1	184.9	7.4
Serro 12	25	11	9.183	0.037	1.099	0.004	74.8	185.7	7.4

Note: Analytical work by M. Brauns. Measurements of reference material JM-Os-DTM yielded an average $^{187}Os/^{188}Os$ ratio of 0.17393 ± 38 (n = 7), which is consistent with published results—e.g., two sets of long-term averages, 0.17429 ± 55 and 0.17396 ± 38 (Shirey, 1997); two sets of averages from Monash University, Australia, 0.17367 ± 58 and 0.17400 ± 21 (Lambert et al., 1998; McBride et al., 2001).

*From ^{190}Pt decay.

TABLE S2. SELENIUM ISOTOPIC VALUES FOR PLATINUM-PALLADIUM NUGGETS FROM CÓRREGO BOM SUCESSO, MINAS GERAIS, BRAZIL.

	Mass (mg)	$\delta^{82/76}$Se (‰)	2 SE (‰)	Pt (wt.%)	Pd (wt.%)	Se (µg g^{-1})	Os (µg g^{-1})	Ir (µg g^{-1})	Tl (µg g^{-1})
Pt-Pd 1	6.32	-17.1	0.04	27.2	12.3	246	0.0295	0.0240	7.71
Pt-Pd 2	18.38	-17.0	0.05	71.6	22.5	1074	0.0603	0.0785	12.3
Pt-Pd 3	16.80	-15.7	0.11	77.9	20.4	1146	0.0389	0.143	28.0
Pt-Pd 4	13.73	-17.0	0.05	84.2	14.7	805	0.0663	0.0781	15.2
Pt-Pd 5*	6.26	-17.4	0.07	92.5	6.18	402	0.128	0.0713	1.43
Pt-Pd 6*	8.12	-16.3	0.07	77.9	19.0	435	n.a.	n.a.	9.90
Pt-Pd 7	4.33	-16.4	0.06	70.3	22.3	801	0.0164	0.0459	16.5
Pt-Pd 8	6.57	-16.6	0.04	n.a.	n.a.	n.a.	n.a.	n.a.	n.a.

Note: Analytical work by M.I. Varas-Reus, B. Eickmann and S. König. Trace elements, originally from Cabral et al. (2019), are listed here as averages of LA–ICP–MS analyses on the same samples.

*Samples dissolved with high-pressure Asher digestion method, all others with hotplate beaker digestion method.

SE: standard error = internal precision of a sample run during Se isotope analysis (over 40 cycles), well within long-term reproducibility (conservatively expressed as ±0.2 ‰, 2 SD) of all previously analyzed samples in our laboratory over a period of 5 years.

n.a.: not analyzed.

TABLE S3. RESULTS OF $\delta^{82/76}$Se (‰) OF THE INTERLABORATORY STANDARD MH−495 (30 ng mL^{-1} Se), MEASURED TOGETHER WITH THE PLATINUM-PALLADIUM NUGGETS

	30 ng mL^{-1} solution	
	$\delta^{82/76}$Se (‰)	2 SE (‰)*
	-3.24	<0.1
	-3.29	<0.1
	-3.07	<0.1
	-3.03	<0.1
	-3.21	<0.1
	-3.24	<0.1
	-3.19	<0.1
	-3.27	<0.1
	-3.26	<0.1
	-3.24	<0.1
	-3.27	<0.1
	-3.27	<0.1
	-3.30	<0.1
	-3.26	<0.1
	-3.28	<0.1
	-3.27	<0.1
	-3.24	<0.1
	-3.32	<0.1
	-3.22	<0.1
	-3.25	<0.1
	-3.08	<0.1
	-3.30	<0.1
	-3.25	<0.1
Average	-3.23	
2 SD	0.15	
	$N = 23$	

*Internal precision of a sample run during Se isotope analysis (over 40 cycles) is reported as 2 standard error (2 SE).

TABLE S4. SELENIUM CONCENTRATIONS AND ISOTOPE COMPOSITIONS OF INTERNATIONAL ROCK REFERENCE MATERIAL USGS (UNITED STATES GEOLOGICAL SURVEY) BCR-2

Sample	Rock type	$\delta^{82/76}$Se (‰)	2 SE (‰)	Se (ng g^{-1})
USGS BCR−2	Basalt	0.04	0.07	79
		0.22	0.06	78
		0.15	0.05	78
		0.13	0.05	77
	Average	0.14		78
	2 SD	0.15		2

Note: Reference material digested and analyzed during the course of this study and that of König et al. (2021).

REFERENCES CITED

Begemann, F., Ludwig, K.R., Lugmair, G.W., Min, K., Nyquist, L.E., Patchett, P.J., Renne, P.R., Shih, C.-Y., Villa, I.M., and Walker, R.J., 2001. Call for an improved set of decay constants for geochronological use: Geochimica et Cosmochimica Acta, v. 65, p. 111–121, doi:10.1016/S0016-7037(00)00512-3.

Birck, J.L., Barman, M.R., and Capmas, F., 1997, Re-Os isotopic measurements at the femtomole level in natural samples: Geostandards Newsletter, v. 20, p. 19–27, doi:10.1111/j.1751-908X.1997.tb00528.x.

Bolea, E., Laborda, F., Belarra, M.A. and Castillo, J.R., 2001, Interferences in electrochemical hydride generation of hydrogen selenide: Spectrochimica Acta Part B: Atomic Spectroscopy, v. 56, p. 2347–2360, doi: 10.1016/S0584-8547(01)00277-4.

Brauns, M., Hergt, J.M., Woodhead, J.D., and Maas, R., 2000, Os isotopes and the origin of the Tasmanian dolerites: Journal of Petrology, v. 41, p. 905–918, doi:10.1093/petrology/41.7.905.

Brauns, M., 2001, A rapid, low-blank technique for the extraction of osmium from geological samples: Chemical Geology, v. 176, p. 379–384, doi:10.1016/S0009-2541(00)00371-5.

Brauns, M., Yahalom-Mack, N., Stepanov, I., Sauder, L., Keen, J., and Eliyahu-Behar, A., 2020, Osmium isotope analysis as an innovative tool for provenancing ancient iron: A systematic approach. PLoS ONE 15, e0229623, doi:10.1371/journal.pone.0229623.

Brookins, D.G., 1988, Eh-pH Diagrams for Geochemistry: Berlin, Springer-Verlag, Berlin, 176 p.

Cabral, A.R., Zack, T., König, S., Eickmann, B., Kwitko-Ribeiro, R., Tupinambá, M., and Lehmann, B., 2019, Distinguishing high- from low-temperature platinum nuggets through their trace-element pattern: Economic Geolology, v. 114, p. 201–206, doi:10.5382/econgeo.2019.4627.

König, S., Eickmann, B., Zack, T., Yierpan, A., Wille, M., Taubald, H., and Schoenberg, R., 2019, Redox induced sulfur-selenium isotope decoupling recorded in pyrite: Geochimica

et Cosmochimica Acta, v. 244, p. 24–39, doi:10.1016/j.gca.2018.09.013.
König, S., Rosca, C., Kurzawa, T., Varas-Reus, M.I., Dragovic, B., Schoenberg, R., and John, T., 2021, Selenium isotope evidence for pulsed flow of oxidative slab fluids: Geochemical Perspectives Letters, v. 17, p. 27–32, doi:10.7185/geochemlet.2110.
Kurzawa, T., König, S., Labidi, J., Yierpan, A., and Schoenberg, R., 2017, A method for Se isotope analysis of low ng-level geological samples via double spike and hydride generation MC–ICP–MS: Chemical Geology, v. 466, p. 219–228, doi:10.1016/j.chemgeo.2017.06.012.
Kurzawa, T., König, S., Alt, J.C., Yierpan, A., and Schoenberg, R., 2019, The role of subduction recycling on the selenium isotope signature of the mantle: constraints from Mariana arc lavas: Chemical Geology, v. 513, p. 239–249, doi:10.1016/j.chemgeo.2019.03.011.
Labidi, J., König, S., Kurzawa, T., Yierpan, A., and Schoenberg, R., 2018, The selenium isotopic variations in chondrites are mass-dependent; implications for sulfide formation in the early Solar System: Earth and Planetary Science Letters, v. 481, p. 212–222, doi:10.1016/j.epsl.2017.10.032.
Lambert, D.D., Foster, J.G., Frick, L.R., Hoatson, D.M., and Purvis, A.C., 1998, Application of the Re-Os isotopic system to the study of Precambrian magmatic sulfide deposits of Western Australia: Australian Journal of Earth Sciences, v. 45, p. 265–284, doi:10.1080/08120099808728386.
McBride, J.S., Lambert, D.D., Nicholls, I.A., and Price, R.C., 2001, Osmium isotopic evidence for crust-mantle interaction in the genesis of continental intraplate basalts from the Newer Volcanics Province, southeastern Australia: Journal of Petrology, v. 42, p. 1197–1218, doi:10.1093/petrology/42.6.1197.
Shirey, S.B., 1997, Re-Os isotopic compositions of Midcontinent rift system picrites: implications for plume-lithosphere interaction and enriched mantle sources: Canadian Journal of Earth Sciences, v. 34, p. 489–503, doi:10.1139/e17-040.
Yierpan, A., König, S., Labidi, J., Kurzawa, T., Babechuk, M.G., and Schoenberg, R., 2018, Chemical sample processing for combined selenium isotope and selenium-tellurium elemental investigation of the Earth's igneous reservoirs: Geochemistry, Geophysics, Geosystems, v. 19, p. 516–533, doi:10.1002/2017GC007299.
Yierpan, A., König, S., Labidi, J., and Schoenberg, R., 2019, Selenium isotope and S-Se-Te elemental systematics along the Pacific-Antarctic ridge: role of mantle processes: Geochimica et Cosmochimica Acta, v. 249, p. 199–224, doi:10.1016/j.gca.2019.01.028.
Yierpan, A., König, S., Labidi, J., and Schoenberg, R., 2020, Recycled selenium in hot spot-influenced lavas records ocean-atmosphere oxygenation: Science Advances, v. 6, eabb6179, doi:10.1126/sciadv.abb6179.